



Introduction to Topology Optimization for the Design of High Voltage Insulators

Balaji Sriram^{1*}, Harivinay Varadaraju² and Nandini Gupta¹

¹Electrical Engineering Department, Indian Institute of Technology Kanpur, Kanpur – 208016, Uttar Pradesh, India; balajis@iitk.ac.in

²Simactricals Private Limited, Kanpur – 208016, Uttar Pradesh, India

Abstract

High Voltage insulators play a vital role in power transmission systems and are subjected to combined electrical, mechanical, and thermal stress. Common design strategies for HV insulators involve semi-analytical methods and Finite Element Analyses (FEA) to arrive at designs that meet the required design and manufacturing criteria. Topology Optimization (TO) is a design strategy widely adopted to minimize the weight and volume of the design while retaining its performance. In this work, we propose a modification to the traditional TO process to maximize the combined electrical and structural performance of HV insulators. This modification incorporates electric field considerations into the T.O. process.

Keywords: Finite Element Analysis, High Voltage Insulators, Topology Optimization

1. Introduction

The reliable operation of power transmission systems heavily depends upon the effectiveness of the High Voltage (HV) insulators which are subject to various stresses including mechanical, electrical, and thermal. The design of HV insulators generally involves semi-analytical methods and/or FEA. This is an iterative approach and might have a long lead time. With recent technological improvements in additive manufacturing, TO can be an effective design strategy for designing HV insulators using less material without impacting performance. This paper adapts the TO strategy to the design of HV insulators. The objective is to minimize the combined electrical and structural stress on a given volume of material, (instead of only concerning structural load). By incorporating the influence of electrostatic fields into the optimization routine, the proposed approach aims to achieve a trade-off between electrical and structural performances resulting in reliable designs for HV insulators at a lower lead time.

This work is limited to computational implementations of topology optimizations using FEA. Experimental validations will be conducted as a part of future studies.

2. Methodology

TO is a computational design strategy used to optimize material distribution within a predetermined design space of interest subject to certain loads and boundary conditions such that the resulting design meets the desired performance specifications. A general TO algorithm is defined as follows.

$$\min_{\mathbf{x}} f(\mathbf{x}), \quad (1)$$

$$s.t., \begin{cases} f_c(\mathbf{x}) \leq \bar{f}_c \forall c=1,2,3,\dots,n_c, \\ 0 \leq \mathbf{x}_e \leq 1 \forall e=1,2,3,\dots,n_e, \end{cases}$$

where $f(\mathbf{x})$ is the objective function and $f_c(\mathbf{x})$, with $c = 1, 2, \dots, n_c$ is constraint functions bound by constraint limits imposed by the function \bar{f}_c and \mathbf{x}_e is the design variable¹.

*Author for correspondence

2.1 Topology Optimization for Static Structural Problems

The structural TO algorithm minimizes the overall compliance of the design subject to a volume constraint. Therefore, Equation (1) may be rewritten as follows.

$$\min_{\mathbf{x}} C_s(\mathbf{x}) = \mathbf{u}^T \mathbf{K} \mathbf{u}$$

$$s.t., \begin{cases} \frac{V(\mathbf{x})}{V_o} = \bar{V}, \\ 0 \leq \mathbf{x}_e \leq 1 \forall e \in \{1, 2, \dots, n_e\}, \end{cases} \quad (2)$$

where, C_s is the structural compliance, \mathbf{u} is the global displacement vector, \mathbf{K} is the global stiffness matrix, $V(\mathbf{x})$ is the current volume fraction, V_o is the maximum volume fraction, \bar{V} is the target volume fraction and \mathbf{x}_e is the elemental density.

2.2 Topology Optimization for Electrostatic Problems

The Field Utilization Factor (FUF) is an important parameter for any insulation system. The higher the FUF, the better the stress control. It is defined as the ratio of an average electric field to the maximum electric field and is given by Equation (3).

$$FUF = \frac{1}{\Omega * \max(F(x))} \int F(x) . dx \forall x \in \Omega, \quad (3)$$

where $F(x)$ is the electric field at the coordinate x in a 3D design space (and not a point on the x -axis). Considering a discretized domain with n_e number of elements, Ω is the region where the material exists in the design space given by Equation (4).

$$\Omega = \{ \mathbf{x}_e \neq 0 \} \forall e \in \{1, 2, 3, \dots, n_e\} \quad (4)$$

In electrostatic TO, the design objective is to maximize FUF (or) to minimize ($-FUF$) subject to a volume constraint following the equation below.

$$\min_{\mathbf{x}} C_{ES}(\mathbf{x}) = -FUF,$$

$$s.t., \begin{cases} \frac{V(\mathbf{x})}{V_o} = \bar{V} \\ 0 \leq \mathbf{x}_e \leq 1 \forall e = 1, 2, \dots, n_e \end{cases} \quad (5)$$

For the sake of simplicity and as a first step the surface stress (creepage stress) is neglected. Therefore, one cannot expect the optimized designs to have sheds, (which are

used to provide sufficient creepage) as that in typical HV insulators.

2.3 Modified SIMP Approach

In this work, a modified Simplified Isotropic Material with Penalisation (SIMP) approach is adopted in the TO algorithm². The SIMP approach modifies the continuous density distribution of the design into a discrete density distribution (either 0 or 1) for obtaining black-and-white regions and ensuring manufacturing feasibility. In the modified SIMP method, each element is assigned a density x_e that determines its Young's modulus E_e as described in the equation below.

$$E_e(x_e) = E_{min} + x_e^p (E_o - E_{min}) \quad (6)$$

where, E_o is the stiffness of the material. Ideally, Young's modulus ' E_e ' of an element 'e' should vary between 0 and E_o as the element density ' x_e ' varies between 0 and 1. However, during static-structural FEA, having Young's modulus equal to zero may result in singular matrix operations^{1,2}. To prevent this issue, a non-zero minimum Young's modulus (usually 10^{-9}) is assigned to elements with no material. With this assumption, Young's modulus of any element varies between E_{min} and E_o as the element density ' x_e ' varies between 0 and 1 following Equation (6). 'p' is the penalty factor (usually assigned to 3). For the electrostatic problem, the formulation is similar. However, the minimum possible relative permittivity is 1 (that of vacuum), therefore modified SIMP equation is written as follows.

$$\epsilon_{r,e}(x_e) = 1 + x_e^p (\epsilon_r - 1) \quad (7)$$

As the element density varies linearly from 0 to 1, the relative permittivity of the element varies non-linearly from 1 to ϵ_r following Equation (7).

2.4 Optimization Routine

The optimization routine follows the Optimality Criteria (OC) method³. The OC method is a popular heuristic approach to solving structural and topology optimization problems. It is an iterative process of sensitivity analysis, update of design variables and filtering until convergence.

2.4.1 Sensitivity Analysis

For the structural case, the sensitivities are computed using the method of adjoint variables. More information

can be found in². Here, the sensitivity of the objective function C_s concerning the design variable x_e is given as follows.

$$\frac{\partial C_s}{\partial x_e} = -p x_e^{(p-1)} (E_o - E_{min}) C_{se}, \quad (8)$$

where, C_{se} is the element of structural compliance. Similarly, the sensitivity of the electrostatic case is given below. A detailed derivation of the same is presented in⁴.

$$\frac{\partial C_{ES}}{\partial x_e} = 2 \varepsilon_{r,e} \frac{\varepsilon_{r,e} - 1}{\varepsilon_{r,e} + 1} F^2(e) \quad (9)$$

where, $F(e)$ is the electric field intensity in the finite element e . The sensitivity of the material volume V concerning x_e is 1 because, the volume in each element increases as much as there is material inside the element^{1,2}.

$$\frac{\partial V}{\partial x_e} = 1 \quad (10)$$

2.4.2 Update of Design Variables

Equation (9) is assumed to govern the evolution of the design variable x_e

$$x_e^{new} = \begin{cases} \max(0, x_e - m) \nabla x_e B_e^n \leq \max(0, x_e - m), \\ \min(0, x_e + m) \nabla x_e B_e^n \geq \min(1, x_e - m) \\ x_e B_e^n \text{ otherwise,} \end{cases} \quad (11)$$

where, m is a positive move limit, n is a numerical damping coefficient set to $\frac{1}{2}$ and B_e is the net structural sensitivity formulated as follows.

$$B_e = \frac{-\frac{\partial C}{\partial x_e}}{\lambda \frac{\partial V}{\partial x_e}}, \quad (12)$$

where, λ is a Lagrangian multiplier chosen to satisfy the volume constraint.

2.4.3 Filtering of Sensitivities

Filtering is implemented into TO routines to ensure continuous solutions, prevent checkerboard patterns and reduce mesh dependency. In this work, a density-based filter is adopted, and it modifies the updated densities as follows⁵.

$$\tilde{x}_e = \frac{1}{\sum_{i \in N_e} H_{ei}} \sum_{i \in N_e} H_{ei} x_i, \quad (13)$$

where, \tilde{x}_e is the filtered density, N_e is the set of elements i for which the center-to-center distance $\Delta(e, i)$ to element e is smaller than the filter radius r_{min} and H_{ei} is the weight factor calculated using the equation below.

$$H_{ei} = \max(0, r_{min} - \Delta(e, i)) \quad (14)$$

2.5 Combined Electrostatic and Static Structural Sensitivities

The overall sensitivity is the weighted sum of the static structural and the electrostatic sensitivities and is expressed as follows.

$$\frac{\partial C}{\partial x_e} = \alpha \frac{\partial C_s}{\partial x_e} + (1 - \alpha) \frac{\partial C_{ES}}{\partial x_e}; 0 \leq \alpha \leq 1 \quad (15)$$

The weight coefficient α is adjusted to control the influence of structural and electrostatic sensitivities in the optimization routine. An increase in α , increases the influence of structural sensitivity and decreases the influence of electrostatic sensitivity in the overall sensitivity following Equation (15). When $\alpha = 0$ the design sensitivity only depends on electrostatic sensitivity. When $\alpha = 1$, the design sensitivity only depends on structural sensitivity. Any other value of α in the range 0 to 1 considers both electrostatic and structural sensitivities.

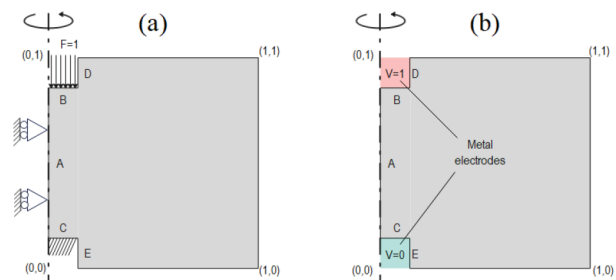


Figure 1. Boundary conditions for (a) static structural FEA and (b) electrostatic FEA.

2.6 Problem Definition

Since, the objective is to optimize the design of HV insulators (which usually have an axis of symmetry), the problem is set up in an R-Z plane (as 2D axisymmetric) as shown in Figure 1. For simplicity, the problem is formulated in a normalized solution domain ranging from $R = 0$ to $R = 1$ and $Z=0$ to $Z=1$. For the same reason, the boundary conditions are also expressed as

nondimensional quantities, specified in normalized units ranging between 0 and 1. The edge A is the axis of symmetry, for both static structural and electrostatic FEA. For static structural FEA, all the nodes on this edge are free to move along the axis but are fixed in the radial direction. HV insulators bear the weight of the HV conductor while being fixed at the other end, experiencing constant compressive stress. Therefore, on edge B, all nodes experience compressive force $F = 1$ in the downward Z direction. All the nodes on the edge C are structurally fixed and immovable as shown in Figure 1(a). For electrostatic FEA, the boundary conditions are displayed in Figure 1(b). A voltage $V = 1$ is applied at all nodes in the HV electrode (pink region) including edges B and D while, the voltage $V = 0$ is applied to all the nodes in the ground electrode (green region) including edges C and E.

3. Results

The domain shown in Figure 1 is discretized into 100×100 elements, r_{min} set to 1.5, the penalty factor p set to 3 and the target volume fraction is set to 20%. This implies that the optimized design will only occupy 20% of the total design space ($R = [0,1]; Z = [0,1]$). The methodology described in the previous section is followed for optimization. FEA is used to solve the governing equations (given below) for static structural and electrostatic problems.

$$K * U = F, \tag{16}$$

$$-\nabla(\epsilon \nabla \Phi) = 0, \tag{17}$$

where, K, U, and F are the global stiffness matrix, global displacement vector and global force vector respectively while ϕ and ϵ are the electrostatic potential and the material permittivity respectively. The computational time for optimization depends on the speed of FEA solutions. Hence a rapid FEA computation routine inspired by the ‘‘MILAMIN’’ project was adopted⁶. This FEA routine can compute solutions in over 20,000 degrees of freedom in less than 0.1 seconds. Further, 3 different designs corresponding to pure electrostatic TO ($\alpha = 0$), pure static structural TO ($\alpha = 1$), and combined TO ($\alpha = 0.5$) having 50% influence of both static structural and electrostatic sensitivities are evaluated. Figure 2(a), (b) and (c) show the design solutions for $\alpha = 0, 0.5$, and 1 respectively. The black regions are the regions occupied by material.

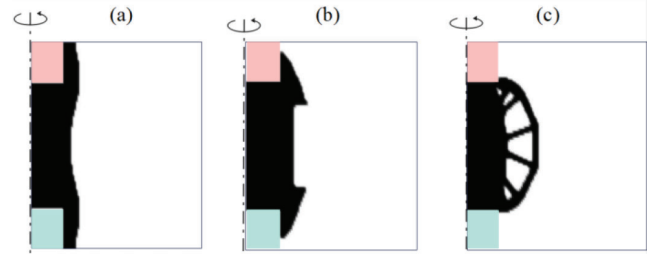


Figure 2. Optimized designs for (a) $\alpha = 0$, (b) $\alpha = 0.5$ and (c) $\alpha = 1$.

The variation of the optimized design with parameter α is significant. However, one factor which is obvious in all cases is that the metal electrodes are always bridged by the material for good structural load bearing capacity as well as electrostatic stress-handling capacity. When $\alpha = 0$, the material fully encloses the electrodes for efficient electrostatic stress control. As α increases to 0.5 the material partially redistributes itself in the region between the metal electrodes to provide a compromise between structural and electrostatic stresses. Also, when $\alpha = 1$ a truss structure is obtained for improved load bearing capacity. Also, due to axis symmetry, the routine preferentially avoids material at the periphery than the material close to the axis of symmetry. To understand the structural integrity of the optimized designs, the combined normal and shear stress also known as the von Mises stress is evaluated for $\alpha = 0, 0.5$ and 1 and is as shown in Figure 3 (a), (b), and (c) respectively.

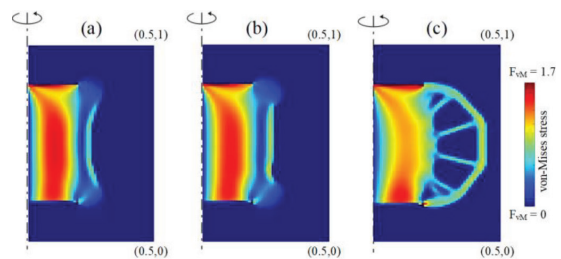


Figure 3. von Mises stress maps inside the optimized designs for (a) $\alpha = 0$, (b) $\alpha = 0.5$ and (c) $\alpha = 1$.

For $\alpha = 0$ case, the material sandwiched between the electrodes is highly stressed whereas, the material enclosing the edges D and E of electrodes contributes to no stress bearing. As α increases to 0.5, the concentration of von Mises stress decreases and the stress is more uniformly distributed throughout the material. When $\alpha = 1$, almost all of the material is subjected to uniform stress. This would limit the corresponding structural deformations for an applied

compressive load. The overall structural compliance for the 3 cases is evaluated and is plotted against α as shown below.

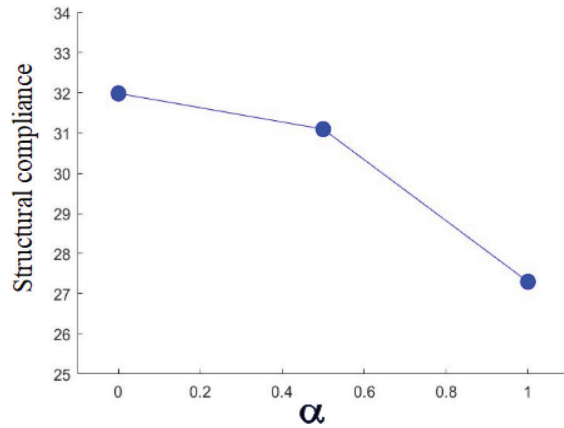


Figure 4. Variation of structural compliance with α .

The variation of structural compliance with α is shown in Figure 4. As expected, with an increase in α , a decrease in structural compliance is observed. This implies that as α increases, the design is less prone to deformations under compressive load. To understand the electrostatic performance of the optimized designs, the electric field intensity maps in the designs for $\alpha = 0, 0.5$ and 1 are evaluated and are displayed in Figure 5 (a), (b), and (c) respectively. The electric field distributions in the material for $\alpha=0$ case are very uniform. However, with an increase in α , the electric field in the material becomes more non-uniform causing disproportionate stress in the material.

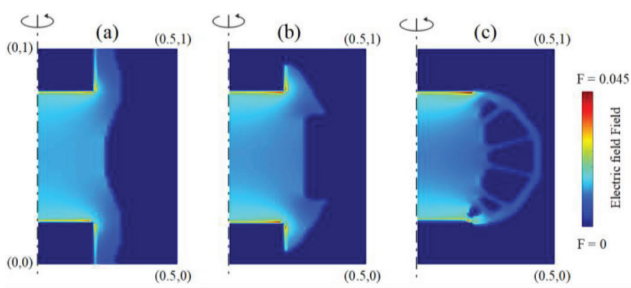


Figure 5. Electric field intensity maps inside the optimized designs for (a) $\alpha = 0$, (b) $\alpha = 0.5$ and (c) $\alpha = 1$.

With the above field results, the FUF is computed using Equation (3) and is plotted against α in Figure 6. From Figure 6, it is observed that an increase in α results in a decrease in FUF. This implies that as α increases, the optimized design exhibits poorer electrostatic stress control and is more prone to failure.

Further, the design obtained in $\alpha = 0.5$ case exhibits improved FUF and decreased compliance compared to cases $\alpha = 0$ and $\alpha = 1$. Therefore, this design ($\alpha = 0.5$) may be regarded as the suitable choice out of the 3 designs.

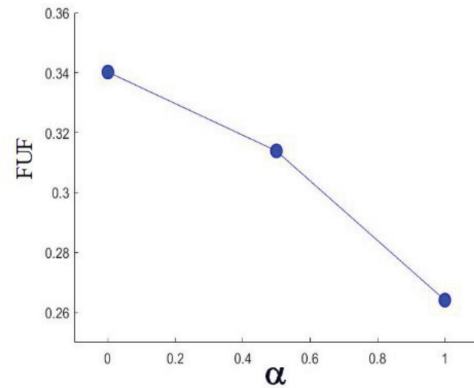


Figure 6. Variation of Field Uniformity Factor (FUF) with parameter α .

4. Conclusion

In the proposed TO procedure, the shape and structure of the material are optimized by considering combined von Mises and electrostatic stress. A weight coefficient α is introduced to adjust the influence of static-structural and electrostatic stresses. When the influence of static-structural stress is neglected ($\alpha=0$), the optimized structure offers the best electrostatic stress control (maximum FUF). When the influence of electrostatic stress is neglected ($\alpha=1$), the optimized structure offers the lowest structural deformations (minimum compliance). When the equal influence of both types of stresses is considered ($\alpha=0.5$), the resultant design offers a perfect balance between structural and electrical design performances. In this process, the optimized designs exhibit reduced von Mises stress concentrations in addition to reduced local electric field enhancements. Experimental validations will be conducted as a part of future work.

5. References

1. Bendsøe MP, Sigmund O. Topology optimization: Theory, methods and applications. Berlin: Springer; 2003. https://doi.org/10.1007/978-3-662-05086-6_2
2. Sigmund O. Morphology-based black and white filters. Structural and Multidisciplinary Optimization. 2007; 33 (4-5):401-24. <https://doi.org/10.1007/s00158-006-0087-x>

3. Bendsøe MP. Optimization of structural topology, shape, and material. Springer; 1995. <https://doi.org/10.1007/978-3-662-03115-5> PMID:8594076
4. Lee KH, Hong SG, Baek MK, Park IH. Hole sensitivity analysis for topology optimization in the electrostatic system using virtual hole concept and shape sensitivity. *IEEE Transactions on Magnetics*. 2016; 52(3):1-4. <https://doi.org/10.1109/TMAG.2015.2499260>
5. Bourdin B. Filters in topology optimization. *International Journal for Numerical Methods in Engineering*. 2001; 50(9):2031-282. <https://doi.org/10.1002/nme.116>
6. Dabrowski M, Krotkiewski M, Schmid DW. Milamin: MATLAB-based finite element method solver for large problems. *Geochemistry, Geophysics, Geosystems*. 2008; 9(4). <https://doi.org/10.1029/2007GC001719>